

# Computational Simulation of Ablation Phenomena in Glass-filled Phenolic Composites

*Aghaaliakbari, Behnaz\*<sup>+</sup>; Jafari Jaid, Abbas; Zeinali, Mir Ali Asghar*

*Iranian Institute of Research and Development in Chemical Industries (IRDICI), Iranian Academic Center for Education, Culture and Research (ACECR), P. O. Box 13145-1494, Tehran, I.R. IRAN*

**ABSTRACT:** *A one-dimensional, transient and thermal degradation model for predicting responses of composite materials when are exposed to the fire is presented. The presented model simulates ablation of composites with different layers of materials and considers material properties as functions of temperature. The reactions are modeled by using Arrhenius-type parameters and density-temperature diagrams which are obtained by specific experimental techniques such as thermogravimetric analysis. This transient thermal model has been implemented in form of a computer code by means of new numerical methods in order to predict the temperature distribution in the liner, the amount of char and erosion, and the liner thickness variations with time. By using implemented computer code, ablation phenomena in a glass-filled phenolic composite has been simulated with the same parameters of a similar experiment. The results are in a good agreement with the experimental data and the model can successfully be used in the design of thermal protection shields as an aid of material and thickness selection.*

**KEY WORDS:** *Ablative composite, Thermal degradation, Heat and mass transfer, Mathematical modeling.*

## INTRODUCTION

In many applications of polymer composites, adequate performance against fire is required. Fire and heat load resistance capabilities of composite materials are mandatory for these applications. The strength of composite materials strongly depends on temperature and rapidly decreases once the temperature exceeds the glass transition temperature. As a result, investigation of structural behavior of composite materials during fires facilitates efficient material design [1-5].

Thermal degradation process is associated with extensive changes in physicochemical properties, and often is endothermic. This process creates gas or liquid

products that are released into the environment. In ablative protection process, heat flux is dissipated by a series of endothermic reactions within the composite. This is followed by substance burning and heat flux reduction. Ablative heat shield operation can be briefly stated as follows: Convective heat which reaches the surface of the composite is balanced with surface radiation, conduction and chemical reactions as shown in Fig. 1. In addition, a large amount of heat flux exerted to the surface by hot exhaust gases, makes this phenomena a destructive process. Ablative composite keeps surface temperature unchanged, and thus, increase in the heat flux

---

\* To whom correspondence should be addressed.

+ E-mail: aghaaliakbari@yahoo.com

1021-9986/15/1/97

10/\$/3.00

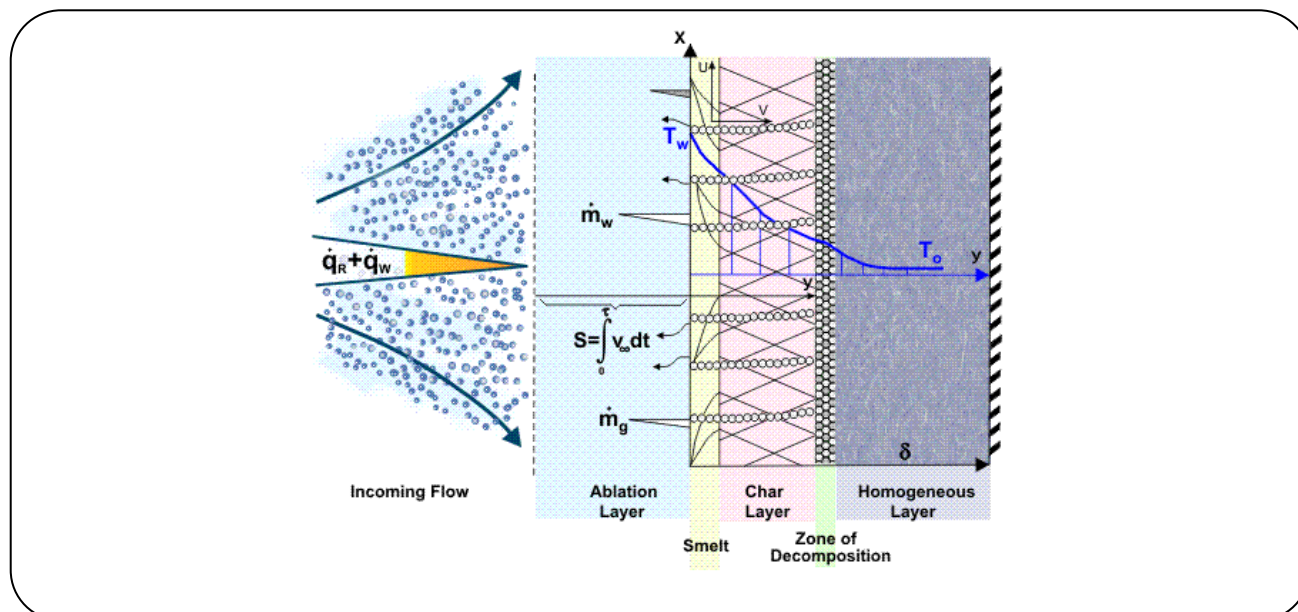


Fig. 1: Graphical representation of ablation phenomena in a composite material [6].

does not affect the temperature of the surface, but intensifies chemical reactions of the process.

Composite thickness should be designed in such a way as to prevent the failure of main structure by keeping back-wall temperature below certain limit, hence it is important to predict the erosion and temperature distribution of the composite during the process. On the other hand, this procedure comprises complex chemical and mechanical processes, so it is difficult to accurately model all of the individual processes. Several analytical models have been developed, which predict the thermal response of the materials during decomposition [6-10]. A thorough review can be found in *Henderson & Wieck* [6].

Generally, degradation modeling is divided into two types: the first type of the modeling is used for simulating of surface ablative protection in which only volume reduces and density remains unchanged, and second type is used for simulating the volume and mixture ablative protection in which density is variable. In this paper, we focus on the second type and model whole system as continuum instead of modeling each zone separately. Moreover, thickness changes during the ablation process complicate the issue. In these circumstances, several techniques have to be adopted in the numerical method.

By adopting innovative modeling and numerical techniques in this paper, most of governing equations numerically are solved without inaccurate assumptions, whereas in previous works, some physical parts

have been neglected or some approximate assumptions have been considered. Additionally, in this paper, system is considered continuum with variable thickness which makes the simulation more complicated while in previous approaches, system has been modeled with different layers or fixed composite thickness. In practice, numerical modeling has been implemented in form of computer code and validation of the code has been checked with benchmarks. Furthermore, this modeling and implemented code has been evaluated with experiments results. This series of experiments have been conducted by *Boyer* [11] on a single fiber-reinforced phenolic material.

## THEORETICAL SECTION

### Mathematical model

In experimental conditions, complex processes of heat and mass transfer take place in the composite. When the composite is exposed to high temperature and high velocity fluid stream, decomposition of resin begins at a pyrolysis temperature and char layer ablation forms at higher temperatures [12]. The free surface of the composite under the influence of high temperature stream is continuously spilled and oxidized.

In this section, the mathematical model which is corresponded to the aforementioned ablation process has been described. Related differential equations, their initial and boundary conditions and equations of composite properties are obtained and presented.

### Governing equations

As the reactions propagate through the composite, the virgin matrix is transformed into the charred substance and finally into the glass. The final glass product is assumed to be non-combustible over the temperature range of the study. The decomposing matrix has only solid and gaseous phases. This implies that the pyrolysis transforms the solid into the gaseous phase directly. These two phases have the same temperature at any given point and the thermal expansion is neglected. Based on these assumptions, the governing equations are [13]:

Conservation of energy for the combined phases:

$$(\rho_a c_a + \rho_c c_c) \frac{\partial T}{\partial t} + \frac{\partial (\dot{m}_g'' h_g)}{\partial x} = \quad (1)$$

$$\frac{\partial}{\partial x} \left( k_e \frac{\partial T}{\partial x} \right) - \left( \frac{\rho_{s0} h_a - \rho_{sf} h_c}{\rho_{s0} - \rho_{sf}} \right) \frac{\partial \rho_s}{\partial t}$$

$$\dot{m}_g''(x, t) = - \int_L^x \left( \frac{\partial \rho_s}{\partial t} \right) ds \quad (2)$$

Conservation of mass for the gas and solid:

$$\frac{\partial \rho_g}{\partial t} + \frac{\partial \dot{m}_g''}{\partial x} = - \frac{\partial \rho_s}{\partial t} = \Lambda \quad (3)$$

And Arrhenius model for the mass source term:

$$\Lambda = \begin{cases} A_1 \rho_{s0} \left[ \frac{\rho_s - \rho_{sf}}{\rho_{s0}} \right]^{n_1} e^{-E/RT} & \text{if } \rho_s > \rho_k \\ A_2 \rho_{s0} \left[ \frac{\rho_s - \rho_{sf}}{\rho_{s0}} \right]^{n_2} e^{-E/RT} & \text{if } \rho_s \leq \rho_k \end{cases} \quad (4)$$

By using mass conservation equation, a relation between location of the composite surface  $s(t)$  and the polymer-char interface can be found:

$$s(t) = s^*(t) + \phi(L - s^*(t)) \quad (5)$$

where  $\phi = y_c(\rho_p/\rho_c)$  is the expansion coefficient.

Since  $s^*$  does not exist in the case of continuity,  $s^*$  (separation location of the two areas with high density difference) can be considered as location of maximum changes in density; In fact, second derivative at this point is zero:

$$\left. \frac{\partial^2 \rho}{\partial y^2} \right|_{y=s^*} = 0 \quad (6)$$

### Boundary and initial conditions

General form of applied initial conditions for the composite is [14]:

$$T(y, t)|_{t=0} = T(y, 0) = T_0 \quad (7)$$

The boundary conditions in general form encompass terms related to convective, radiative and blowing exchange at the free composite surface. The amount of energy transferred to the composite, which leads to increase in the temperature of the sample and its thermal degradation, can be obtained from the following equation:

$$q_k = q_e - q_{rw} - q_{bl} - q_w \quad \text{at } x = s_1(t) \quad (8)$$

In Eq. (8),  $q_k$  is amount of conductive heat transfer,  $q_e$  is amount of convective heat flux transferred from surrounding into the surface and  $q_{bl}$ ,  $q_{rw}$  and  $q_w$  are the convective heat flux injected into the surface boundary, the radiation heat flux radiated to the surrounding and convective heat flux injected into the high temperature wall, respectively [15].

The amount of heat transfers are determined by the following equations:

$$q_k = -K \frac{\partial T}{\partial y} \quad (9)$$

$$q_e = h(T_e - T_0) \quad (10)$$

$$q_{rw} = \epsilon \sigma T_w^4 \quad (11)$$

$$q_w = C_p(I)(T_w - T_0) \quad (12)$$

$$q_{bl} = \gamma_{bl} G(I)^{-1} (q_e - q_w); \quad \gamma_{bl} = 0.7 \left( \frac{M_{wg}}{16} \right)^{0.55} \quad (13)$$

$$G = \left( \frac{J_m^0 \Gamma_m k_m}{c_m} \right)^{1/2} \left( \frac{RT_w}{E_{am}} \right)^{1/2} \exp \left( - \frac{E_{am}}{2RT_w} \right) \quad (14)$$

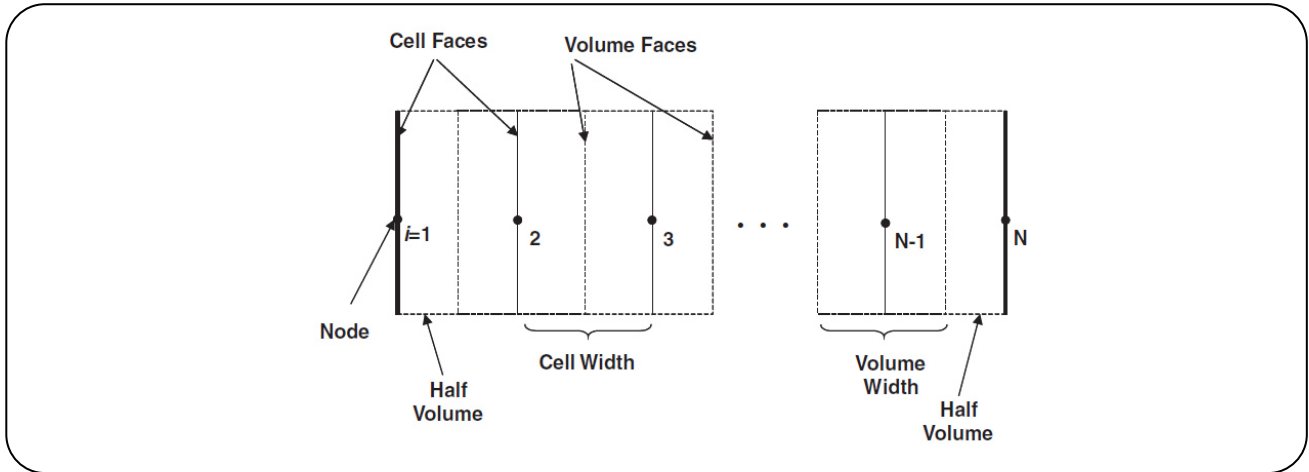


Fig. 2: Details of the gridding.

### Composite properties

According to continuous properties of the composite, density can be considered as Eq. (15):

$$\rho_s = \rho_a + \rho_c \quad (15)$$

Subscripts 'a' and 'c' are related to primary composite and solid phase of reaction products, respectively. By using mass fraction averaging for the solid enthalpy,

$$h_s = Y_a h_a + Y_c h_c \quad \text{where} \quad Y_a = \frac{\rho_a}{\rho_s} \quad \text{and} \quad Y_c = \frac{\rho_c}{\rho_s} \quad (16)$$

$$\rho_s h_s = \rho_a h_a + \rho_c h_c \quad (17)$$

$$\frac{\partial(\rho_a h_a + \rho_c h_c)}{\partial t} + \frac{\partial(\dot{m}_g'' h_g)}{\partial x} = \frac{\partial}{\partial x} \left( k_e \frac{\partial T}{\partial x} \right) \quad (18)$$

To identify the density of each component by using the density of composite, the following relationships are used:

$$\rho_s = \rho_{s0} \left| \frac{\rho_s - \rho_{sf}}{\rho_{s0} - \rho_{sf}} \right| \quad (19)$$

$$\rho_c = \rho_{sf} \left| \frac{\rho_{s0} - \rho_s}{\rho_{s0} - \rho_{sf}} \right| \quad (20)$$

where  $\rho_{s0}$  and  $\rho_{sf}$  are initial and final density of composite, respectively. Therefore:

$$\frac{\partial \rho_a}{\partial t} = - \left[ \frac{\rho_{s0}}{\rho_{s0} - \rho_{sf}} \right] \Lambda \quad \rho_{a0} = \rho_{s0} \quad (21)$$

$$\frac{\partial \rho_c}{\partial t} = - \left[ \frac{\rho_{sf}}{\rho_{s0} - \rho_{sf}} \right] \Lambda \quad \rho_{c0} = 0 \quad (22)$$

Additionally, to obtain effective thermal conductivity, the following equation is used:

$$k_e = \frac{\rho_a \rho_{sf} k_a + \rho_c \rho_{s0} k_c}{\rho_a \rho_{sf} + \rho_c \rho_{s0}} \quad (23)$$

### Numerical model with moving grid

As mentioned above, this modeling has a moving boundary at the top of the sample, which makes it more complex. In this model, the composite has been divided into the layers with a node at the center of each layer as shown in Fig. 2 [16]. As the char layer erodes, thickness of the outer layer decreases which makes the simulation arduous. To handle this situation, the number of layers is kept fixed but the layers thickness is updated after each time step. Furthermore after each time step, the solution values at the new arranged points are interpolated from values of old mesh points.

On the other hand, the spectral method is used to solve differential equations. This method is used to find the smooth with negligible fluctuations.

### Spectral method

Spectral method is one of the most capable methods used to solving complicated partial differential equations. The main idea of this method is considering the solution of equations as sum of orthogonal functions (such as Fourier and Chebyshev functions) whereas coefficients of these functions are unknown. In order to find unknown

variables, it is necessary to solve the same number of equations. So, a few points equal to the number of unknown variables are considered in the domain. For each point, governing equations are applied to the assumed solution. Since the solution is sum of series of simple functions, operations (such as integral and derivation) in the equations can be applied easily.

In this method, type and number of orthogonal functions should be specified. In this paper, Chebyshev functions are selected for this purpose and number of functions is determined with respect to the required accuracy for each case. In the following, Chebyshev functions and numerical approach are introduced.

Since Chebyshev functions are orthogonal polynomials, computing derivative, integrals and mathematical operations can be done with high speed. These polynomials are defined by recursion as follows:

$$T_0(x) = 1, T_1(x) = x, T_{n+1}(x) = 2xT_n(x) - T_{n-1}(x) \quad (24)$$

#### Solution of ODE

In Eq. (1), T is an unknown variable which must be calculated. Generally, T(x,t) is a function of location and time, however by solving this equation in each time step, T can be considered as a function of location only and some terms such as  $\frac{\partial T}{\partial t}$  can be obtained by previous time step solution:

$$\left. \frac{\partial T(x,t)}{\partial t} \right|_t = \frac{T(x) - T_{old}(x)}{\Delta t} \quad (25)$$

So the function T(x) (which is function of location only) can be written as a sum of Chebyshev orthogonal functions. In this case, assume that order of accuracy is n+1, so T(x) is considered as sum of n+1 Chebyshev function. Thus:

$$T(x) = \sum_{i=0}^n c_n F_n(x) \quad (26)$$

In Eq. (26), temperature is considered as sum of multiplication of Chebyshev functions ( $F_n$ ) and at the beginning of the procedure, this coefficients are unknown and can be found by solving system of equations.

Additionally, best efficiency and result approximation of Chebyshev functions are in the range [-1,1], while

composite thickness is variable and equations must be solved in domain  $x \in [a, b]$ . So a linear mapping should be considered between these two ranges:

$$y: [-1, 1], x: [a, b] \quad (27)$$

$$y = \frac{2}{b-a}x - \frac{b+a}{b-a}$$

Thus, Eq. (26) can be corrected as follows:

$$T(x) = \sum_{i=0}^n c_n F_n(Ax + B), A = \frac{2}{b-a}, B = \frac{b+a}{b-a} \quad (28)$$

By using Eqs. (1) and (28), following result is obtained:

$$\sum_{i=0}^n c_i \left( k_e A^2 F_i''(Ax + B) - F_i'(Ax + B) / \Delta t \right) = \quad (29)$$

$$\left( \frac{\rho_{s0} h_a - \rho_{sf} h_c}{\Delta t} \right) \frac{\partial \rho_s}{\partial t} + \frac{\partial (\dot{m}_g h_g)}{\partial x} - (\rho_a c_a - \rho_c c_c) \frac{T_{old}(x)}{\Delta t}$$

To create the system of equations, location of n+1 points must be determined. Two equations are related to the boundary conditions at the beginning and end of the range, and the rest (n-1 points) are within the range. The points are located uniformly throughout the solution domain and by using Eq. (29), n-1 equations are obtained.

To complete the system of equations, it is sufficient to create two equations that are related to the boundary conditions. In case of constant temperature conditions, these equations are:

$$T(0) = T_c \quad (30)$$

$$\sum_{i=0}^n c_n F_n(B) = T_c \quad (31)$$

And in case of adiabatic boundary conditions:

$$\left. \frac{\partial T}{\partial x} \right|_{x=0} = 0 \quad (32)$$

$$\sum_{i=0}^n c_n A F_n'(B) = 0 \quad (33)$$

Equation of boundary condition in case of heat transfer with different ways such as radiation and convection heat is:

Table 1: Values of test parameters.

$T_\infty = T_0 = 297.15 \text{ K}, T_a^0 = T_c^0 = T_g^0 = 293.15 \text{ K}$
$h_a^0 = -552 \text{ kJ/kg}, h_c^0 = 0, h_g^0 = 0$
$k_a = 0.453 + 10210/T^{1.5}, 273.15 \text{ K} \leq T \leq 873.15 \text{ K}, [k_a \text{ in W/(mK)}, T \text{ in K}]$
$k_c = 0.3736 + 4.017 \times 10^{-4} T, 273.15 \text{ K} \leq T \leq 873.15 \text{ K}, [k_c \text{ in W/(mK)}, T \text{ in K}]$
$c_a = 285.2 + 3.565T, 273.15 \text{ K} \leq T \leq 873.15 \text{ K}, [c_a \text{ in J/(kg K)}, T \text{ in K}]$
$c_c = 518.96 + 0.736T, 273.15 \text{ K} \leq T \leq 873.15 \text{ K}, [c_c \text{ in J/(kg K)}, T \text{ in K}]$
$c_g = 3109 \text{ J/(kg K)}$
$h_a = -788789 + 285.2T + 1.7825T^2, 273.15 \text{ K} \leq T \leq 873.15 \text{ K}, [h_a \text{ in J/kg}, T \text{ in K}]$
$h_c = -183785 + 518.96T + 0.368T^2, 273.15 \text{ K} \leq T \leq 873.15 \text{ K}, [h_c \text{ in J/kg}, T \text{ in K}]$
$h_g = -911403 + 3109T, 273.15 \text{ K} \leq T \leq 873.15 \text{ K}, [h_g \text{ in J/kg}, T \text{ in K}]$
$\rho_{s0} = 1700 \text{ kg/m}^3, \rho_{sf} = 1120 \text{ kg/m}^3, \rho_k = 1598 \text{ kg/m}^3$
$n_1 = 55.4, n_2 = 3.81$
$A_1 = 6.78 \times 10^{44} \text{ Hz}, A_2 = 1.3 \times 10^{16} \text{ Hz}, E = 2.18 \times 10^8 \text{ J/kmol}$
$\varepsilon_0 = 0.9, h_0 = 0, \varepsilon_N = 0.9, h_N = 10 \text{ W/m}^2$

$$-k \frac{\partial T_s}{\partial n} = \left\{ h_f + h_r (T_s^2 + T_\infty^2) (T_s + T_\infty) \right\} (T_s - T_\infty) + \quad (34)$$

$\phi_s(x_s, t)$

Due to the nonlinear nature of the obtained relation, in some terms,  $T_s$  is substituted with its value in the previous time step:

$$-kc_n A_n F_n (Ax_s + B) = \quad (35)$$

$$\left\{ h_f + h_r (T_{s,t-1}^2 + T_\infty^2) (T_{s,t-1} + T_\infty) \right\} \times$$

$$(C_n F_n (Ax_s + B) - T_\infty) + \phi_s(t)$$

$$C_n F_n (Ax_s + B) \times \quad (36)$$

$$\left( kA_n + \left\{ h_f + h_r (T_{s,t-1}^2 + T_\infty^2) (T_{s,t-1} + T_\infty) \right\} \right) =$$

$$T_\infty \left\{ h_f + h_r (T_{s,t-1}^2 + T_\infty^2) (T_{s,t-1} + T_\infty) \right\} - \phi_s(t)$$

After obtaining the necessary equations to solve the system of equations, the matrix of equations will be as follows:

$$Ac = b, \quad c = \begin{bmatrix} c_0 \\ c_1 \\ \vdots \\ c_n \end{bmatrix} \quad (37)$$

That  $c$  is matrix of unknown coefficients of solution and elements of matrix  $A$  and  $b$  can be achieved by obtaining general governing equations and boundary conditions that have been mentioned earlier. This system of equations can be solved by Gaussian elimination technique.

## RESULTS AND DISCUSSION

The experimental measurements of tests 07,09 and 10 conducted by Boyer [11] have been reproduced by using the explained model. In these experiments, a glass-filled phenolic composite (MXBE-350) designed by fiberite corporation has been exposed to the heat. The heat fluxes in experiments are given in Fig. 3. Detailed experimental data by using Arrhenius kinetics model are given in Table 1. These data have been derived from reference [13] with the exceptions of the initial, ambient, and reference temperatures and the emissivity, which are not stated in this reference.

In each of these tests, amount and duration of inlet heat which has been applied to the composite is different. Duration of tests 07 and 09 are 105 seconds and test 10 is 225 seconds. In addition, amount of input heat is shown in Fig. 3. Due to different amount of applied heat, comparison of the test results is possible. In this case, by using implemented software, results are examined in three cases:

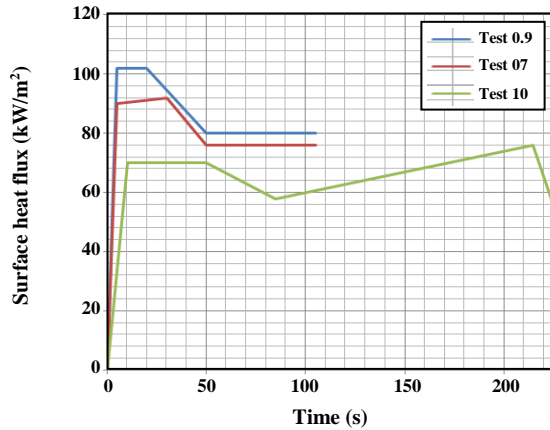


Fig. 3: Piecewise linear approximations of the heat fluxes measured by Reference [11].

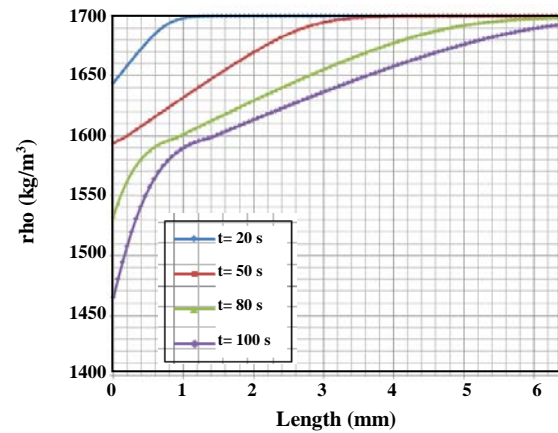


Fig. 5: Density of the domain in various times in test 07.

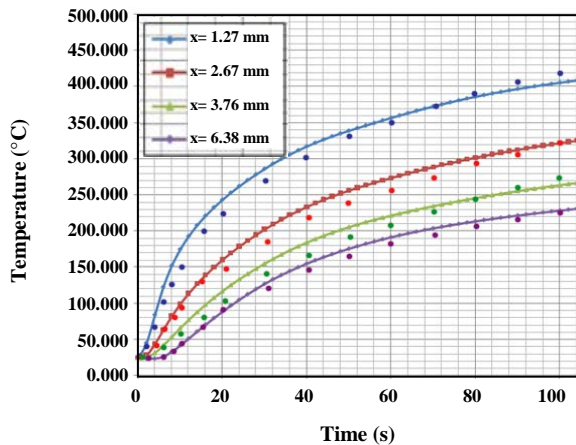


Fig. 4: Comparison of temperature changes at some point during the ablation process in test 07.

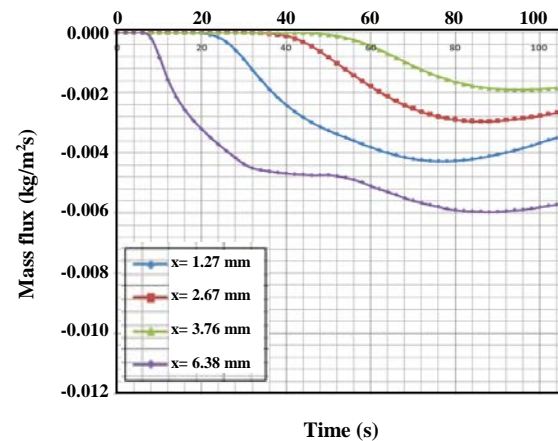


Fig. 6: Mass flux through the different stages of composite during the ablation process in test 07.

- 1- Temperature changes at different sections of composite during the ablation process
- 2- Density of the domain in various times
- 3- Mass flux through different sections of composite during the ablation process

In Fig. 4, temperature changes at different sections during ablation process in test 07 are shown. As Fig. 4 shows, computer results are in good agreement with the experimental data which indicates this computational method is highly predictive. At the beginning of simulation, temperatures of all sections are equal to the ambient temperature and after heating temperature of each section increases. Additionally, rates of temperature changes in sections near the boundary are higher. This means that reactions near heat source are more active and char materials are created in this area at initial stage.

Density of the domain in various times and mass flux through the different sections of composite during the ablation process in test 07 are illustrated in Figs. 5 and 6, respectively.

In Fig. 5, at the beginning of heating process, density of the domain is identical and after some time, due to conversion of composite to char, density of areas close to heat source decreases rapidly and this reduction continues until the conversion of material occurs entire the domain. Fig. 6 illustrates mass flux (due to releasing gas products of reactions) through the domain in different instants. At first stage of process, mass fluxes increase (because of onset of reactions) and after a while, these fluxes decrease. The reason of mass flux reduction is that most of material conversion occurs and reactant is not suffice to continue reactions.

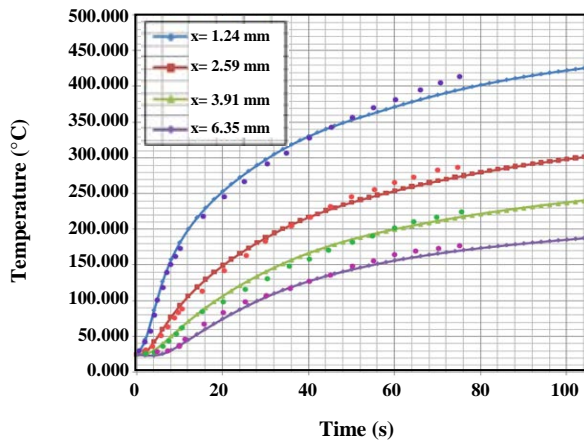


Fig. 7: Comparison of temperature changes at some point during the ablation process in Test 09.

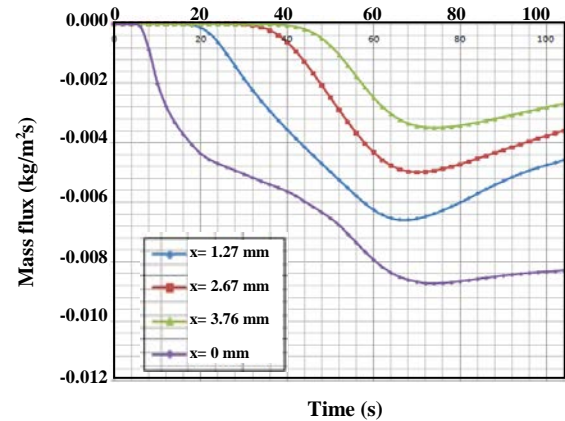


Fig. 9: Mass flux through the different stages of composite during the ablation process in Test 09.

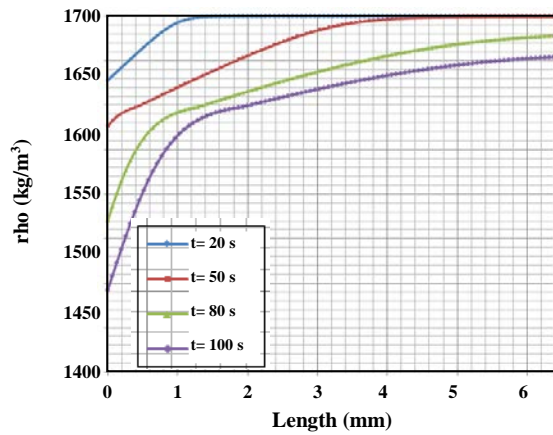


Fig. 8: Density of the domain in various times in Test 09.

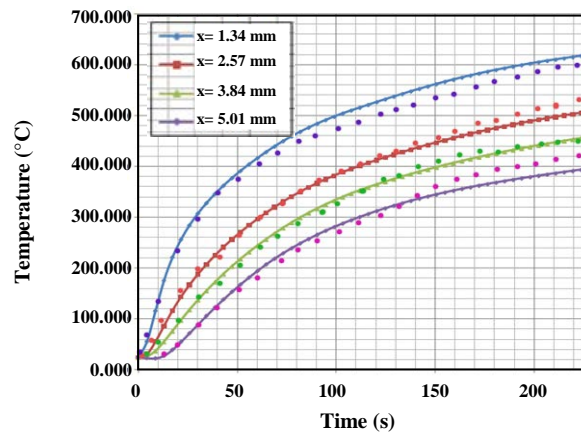


Fig. 10: Comparison of temperature changes at some point during the ablation process in Test 10.

In Fig. 7, temperature changes at some point during ablation process Test 09 is shown. Furthermore, density of the domain in various times and mass flux through the different sections of composite during the ablation process in Test 09 are illustrated in Figs. 8 and 9, respectively.

In Fig. 10, temperature changes at some points during ablation process in Test 10 are shown. Good agreement between computational results and experimental results is apparent. Density of the domain in various times and mass flux through the different sections of composite during the ablation process in Test 10 are illustrated in Figs. 11 and 12, respectively.

As mentioned in modeling section of this paper,  $y_c$  is an experimental value that is effective on erosion of composite. For simplification, this variable is considered

constant in different temperatures. Hence, in order to observe the influence of this parameter on erosion, different values are considered for this parameter. Fig. 13 shows that as  $y_c$  increases, rate of erosion of composite decreases.

**CONCLUSIONS**

An ablative model for predicting responses of composite materials when are exposed to heat source presented and mathematical, physical and chemical aspects of this model was investigated. In order to simulate this phenomenon, numerical method and innovative techniques were introduced and procedure of implementation was mentioned. Finally, in order to verify implemented predictive computational tool, results of the software were compared with experimental results.

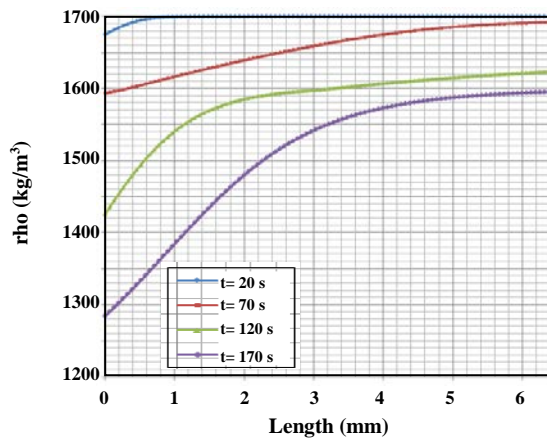


Fig. 11: Density of the domain in various times in Test 10.

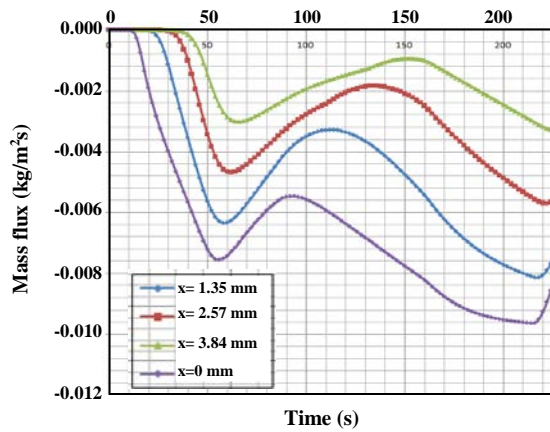


Fig. 12: Mass flux through the different stages of composite during the ablation process in Test 10.

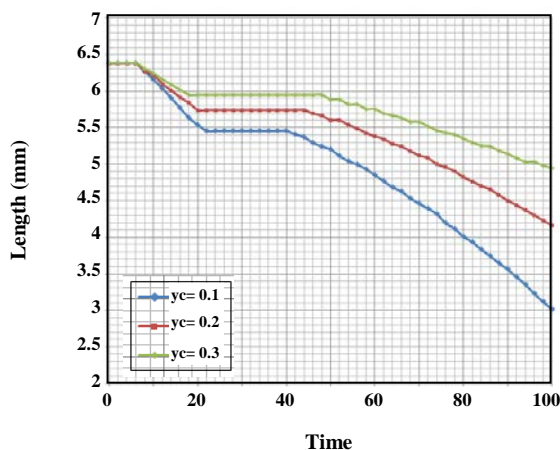


Fig. 13: Thickness changes in composite with different  $y_c$ .

Investigated results were consists of temperature changes at different sections of composite, density distribution of the domain in various times and mass flux through different sections of composite during the ablation process. These case studies were done and illustrated that the developed one-dimensional model provides the predictions very close to the experimental results. The discrepancies between the predicted and the experimental results are thought to be due to the fact that the model does not account for all of the physical processes which occur in the material. In addition, the material properties play a vital role in the accuracy of the results, and any inaccuracy in some of the material properties could account for part of the discrepancy. In a nutshell, the mathematical model could be further improved by including the processes mentioned above.

### Nomenclature

$\rho$	Density
$c$	Specific heat capacity
$T$	Temperature
$T_a$	Ambient temperature
$t$	Time
$k$	Thermal conductivity
$h$	Enthalpy
$\dot{m}''$	Mass flux
$R$	Universal gas constant
$E$	Activation energy
$L$	Composite thickness
$s$	Char moving boundary
$s^*$	Pyrolysis moving boundary
$I$	Enthalpy of surrounding hot gas

Received : Jan. 13, 2014 ; Accepted : Jan. 19, 2015

### REFERENCES

- [1] Henline, William D., *Thermal Protection Analysis of Mars-Earth Return Vehicles*, *Journal of Spacecraft and Rockets*, **29**(2): 198-207 (1992).
- [2] Fang, Yiqun, et al., Effect of Zinc Borate and Wood Floor on Thermal Degradation and Fire Retardancy of Polyvinyl Chloride (PVC) Composites, *Journal of Analytical and Applied Pyrolysis*, **100**: 230-236 (2013).

- [3] Dhakal H.N., Zhang Z.Y., Nick Bennett, [Influence of Fibre Treatment and Glass Fbrehybridisation on Thermal Degradation and Surface Energy Characteristics of Hemp/Unsaturated Polyester Composites](#), *Composites, Part B: Engineering* **43**(7): 2757-2761 (2012).
- [4] Liao, Hui Wei, et al. [Study on Catalysis of Cu-Fe Metal Composite Oxides to Thermal Decomposition Behavior of Bluestone](#), *Iran. J. Chem. Chem. Eng. (IJCCE)*, **30**(2): 33-39 (2011).
- [5] Matsuyama, Shingo, et al., [Numerical Simulation of Galileo Probe Entry Flow Field with Radiation and Ablation](#), *Journal of Thermophysics and Heat Transfer*, **19**(1): 28-35 (2005).
- [6] Henderson J.B., Wiecek T.E., [A Mathematical Model to Predict the Thermal Response of Decomposing, Expanding Polymer Composites](#), *Journal of Composite Materials*, **21**(4): 373-393 (1987).
- [7] McManus, Hugh L.N., George S. Springer, [High Temperature Thermomechanical Behavior of Carbon-Phenolic and Carbon-Carbon Composites, i. Analysis](#), *Journal of Composite Materials* **26**(2): 206-229 (1992).
- [8] Staggs J.E.J., [A Theoretical Appraisal of the Effectiveness of Idealised Ablative Coatings for Steel Protection](#), *Fire Safety Journal*, **43**(8): 618-625 (2008).
- [9] Wang, Xin et al., [Flame Retardancy and Thermal Degradation Mechanism of Epoxy Resin Composites Based on a DOPO Substituted Organophosphorus Oligomer](#), *Polymer*, **51**(11): 2435-2445 (2010).
- [10] Matting, Fred W. ["Analysis of Charring Ablation with Description of Associated Computing Program"](#), National Aeronautics and Space Administration (1970).
- [11] Boyer, Charles Thomas, ["An Analytical and Experimental Investigation of the Thermophysical Properties of a Swelling, Charring Composite Material"](#), Diss. Virginia Polytechnic Institute and State University (1984).
- [12] Bai, Yu, Thomas Keller, [Modeling of Strength Degradation for Fiber-Reinforced Polymer Composites in Fire](#), *Journal of Composite Materials*, **43**(2): 2371-2385 (2009).
- [13] Trelles, Javier, Brian Y. Lattimer, [Modelling Thermal Degradation of Composite Materials](#), *Fire and Materials*, **31**(2): 147-171 (2007).
- [14] Bahramian A.R., et al. [Ablation and Thermal Degradation Behaviour of a Composite Based on Resol Type Phenolic Resin: Process Modeling and Experimental](#), *Polymer*, **47**(10): 3661-3673 (2006).
- [15] Jawaid M., Abdul Khalil H.P.S., [Effect of Layering Pattern on the Dynamic Mechanical Properties and Thermal Degradation of Oil Palm-Jute Fibers Reinforced Epoxy Hybrid Composite](#), *BioResources*, **6**(3): 2309-2322 (2011).
- [16] Childs K.W. ["HEATING 7: Multidimensional, Finite-Difference Heat Conduction Analysis Code System"](#), *Version 7.3. RSICC Report PSR 199* (1998).